β_2- but not β_1-adrenoceptor activation modulates intracellular oxygen availability

Jun Li[1,2,3], Biao Yan[1,4], Zhaoxia Huo[1,4], Ying Liu[1,4], Jiahong Xu[2], Yunfu Sun[5], Yi Liu[1,3], Dandan Liang[1,3], Luying Peng[1,3], Youyi Zhang[6], Zhao-Nian Zhou[7], Jingyi Shi[8], Jianmin Cui[8] and Yi-Han Chen[1,2,3]

[1]*Key Laboratory of Arrhythmias, Ministry of Education, China (East Hospital, Tongji University School of Medicine), Shanghai 200120, China*
[2]*Department of Cardiology, East Hospital, Tongji University School of Medicine, Shanghai 200120, China*
[3]*Institute of Medical Genetics, Tongji University, Shanghai 200120, China*
[4]*Department of Biochemistry and Molecular Biology, School of Life Science and Technology, Tongji University, Shanghai 200092, China*
[5]*School of Pharmacy and Pharmaceutical Sciences, University of California at San Diego (UCSD), 9500 Gilman Drive, La Jolla, CA 92093-0613C, USA*
[6]*Key Laboratory of Molecular Cardiovascular Sciences, Ministry of Education and Institute of Vascular Medicine, Third Hospital, Peking University, Beijing 100083, China*
[7]*Laboratory of Hypoxic Cardiovascular Physiology, Shanghai Institutes for Biological Sciences, Chinese Academy of Sciences, Shanghai 200031, China*
[8]*Department of Biomedical Engineering and Cardiac Bioelectricity and Arrhythmia Centre, Washington University, 1 Brookings Drive, St Louis, MO 63130, USA*

β-Adrenoceptors (β-ARs) play a critical role in the regulation of cardiovascular function. Intracellular oxygen homeostasis is crucial for the survival of cardiomyocytes. However, it is still unclear whether β-AR activation can modulate intracellular oxygen. Here we used mitochondrial and cytosolic target *Renilla* luciferase to detect intracellular oxygen concentration. Pharmacological experiments revealed that β_2-AR activation specifically regulates intracellular oxygen in cardiomyocytes and COS7 cells. This effect was abrogated by inhibitory G protein (G_i) inhibition, endothelial nitric oxide synthase (eNOS) blockade, and NO scavenging, implicating that the β_2-AR–G_i–eNOS pathway is involved in this regulation. β_2-AR activation increased the AMP/ATP ratio, AMPK activity, ROS production and prolyl hydroxylase activity. These effects also contribute to the regulation of β_2-AR signalling, thus providing an additional layer of complexity to enforce the specificity of β_1-AR and β_2-AR signalling. Collectively, the study provides novel insight into the modulation of oxygen homeostasis, broadens the scope of β_2-AR function, and may have crucial implications for β_2-AR signalling regulation.

(Received 2 April 2010; accepted after revision 11 June 2010; first published online 14 June 2010)
Corresponding author Y.-H. Chen: Key Laboratory of Arrhythmias, Ministry of Education, China (East Hospital, Tongji University School of Medicine), 150 Jimo Road, Shanghai 200120, China. Email: yihanchen@tongji.edu.cn

Abbreviations AMPK, AMP-activated kinase; β-AR, β-adrenoceptor; DAF-2, 4,5-diaminofluorescein; eNOS, endothelial nitric oxide synthase; G_i, inhibitory G protein; GPCRs, G protein-coupled receptors; H_2DCFDA, dichlorodihydrofluorescein diacetate; iNOS, inducible NO synthase; ISO, isoproterenol (isoprenaline); nNOS, neuronal NO synthase; NO, nitric oxide; PHD, prolyl hydroxylase; P_{O_2}, partial pressure of oxygen; PTX, pertussis toxin; ROS, reactive oxygen species.

Introduction

Oxygen homeostasis represents an essential organizing principle of metazoan evolution, development, physiology and pathology (Semenza, 2007*a*). In the normal physiological state, the majority of cellular oxygen consumption occurs in the mitochondria for the generation of sufficient ATP to satisfy cellular energy requirements. However, there is also a critical level of 'spare' oxygen available to facilitate the activity of non-mitochondrial dioxygenases elsewhere in the cell (Taylor, 2008*a*). A rapid change in cellular oxygen can act as the initial signal to activate the appropriate pathway to combat external stimuli (Taylor, 2008*b*).

β-Adrenoceptors (β-ARs) are prototypical G protein-coupled receptors (GPCRs) that play a critical role in the regulation of cardiovascular and pulmonary function as well as in other physiological processes (Johnson,

Jun Li, Biao Yan, Zhaoxia Huo and Ying Liu contributed equally to this work.

DOI: 10.1113/jphysiol.2010.190900

1998; Rockman *et al.* 2002). β-AR dysfunction is a cause of cardiovascular and respiratory impairment and a consequence of agonist therapy (Insel, 1996). In particular, loss of β-AR responsiveness is causally linked to both asthma (Johnson, 1998) and heart failure (Lefkowitz *et al.* 2000) as well as to the morbidity and mortality associated with the therapeutic use of β-agonists (Salpeter *et al.* 2004). Thus, it is necessary to fully understand β-AR function.

β-AR activation can enhance bronchodilatation and alveolar fluid clearance (which increase O_2 uptake), increase cardiac output and peripheral vasodilatation (which increase O_2 delivery), and enhance cardioprotection and angiogenesis under ischaemic conditions (Lefkowitz *et al.* 2000; Iaccarino *et al.* 2002; Mieno *et al.* 2005; Iaccarino *et al.* 2005). Such research has mainly focused on β-AR activation at the tissue or organ level. However, oxygen changes that occur at the subcellular level in response to various stimuli have not been studied to date. In this study, we explored the relationship between β-AR activation and intracellular oxygen in cardiomyocytes, revealing that β_2-ARs selectively increase intracellular oxygen availability through the β_2-AR–G_i–eNOS signalling pathway.

Methods

Plasmids

Mitochondrial targeted *Renilla* luciferase (MitRLuc) and cytosolic *Renilla* luciferase (pRL-CMV) plasmids for detecting intracellular oxygen concentration were generously provided by Dr Thilo Hagen and Salvador Moncada (Wolfson Institute for Biomedical Research, University College London, London, UK). The mitochondria-target or cytosol-target *Renilla* luciferase sequence was obtained from MitRLuc-pcDNA3 or pRL-CMV plasmids, respectively, and then cloned into pLenti6 V5-D to generate pLenti6-V5/MitRLuc or pLenti6-V5/Rluc for cardiomyocyte transfection. The specific protocol for lenti-viral vector construction is shown in the Supplemental material (available online only). β_1-AR and β_2-AR plasmids were gifts from Dr Kenneth P. Minneman (Emory University School of Medicine, Atlanta, GA, USA). The pST39-HisTrxNVHL-elongin B-elongin C plasmid was kindly provided by Dr S. Tan (Pennsylvania State University, PA, USA).

Neonatal rat cardiomyocyte isolation

All procedures for animals were approved by the Animal Ethics and Experimentation Committee of Tongji University (Shanghai, China) and were performed in accordance with the *Guide for the Care and Use of Laboratory Animals* published by the US National Institutes of Health (NIH Publication No. 85-23, revised 1996) as well as in compliance with the report of the policies and regulations on animal experimentation (Drummond, 2009). One-day-old Sprague–Dawley rats were anaesthetized by inhalation of 2% isoflurane (99.9% from Vedco, St Joseph, MO, USA). The hearts of the neonatal rats were rapidly excised with sharp scissors and then washed with ice-cold PBS (mmol l^{-1}: NaCl 136.9, KCl 2.7, Na_2HPO_4 8.1 and KH_2PO_4 1.5, pH 7.3) to remove blood and debris. After removing the connective tissue, blood vessels and the atria, the ventricles were rapidly minced and incubated in a PBS solution containing trypsin (0.2%), collagenase (0.1%) and glucose (0.02%) for 30 min at 37°C. The myocardial cells were then isolated by repeat pipetting of the digested myocardial tissue. The cells in the supernatant were transferred into a tube containing culture medium (Dulbecco's modified Eagle's medium containing 10% fetal bovine serum, 0.1 mmol l^{-1} β-mercaptoethanol, and 100 U ml^{-1} penicillin and 100 μg ml^{-1} streptomycin). The tube was centrifuged at 600 *g* for 5 min at room temperature, and the cell pellet was re-suspended in the culture medium. Isolated cells were purified by pre-plating for 30 min to reduce the number of non-myocytes. Bromodeoxyuridine (0.1 mmol l^{-1}) was also added to prevent the growth of fibroblasts. Cardiomyocyte purity was approximately 95%, as assessed by microscopic observation of cell beating.

Preparation of mitochondrial fractions

Cells were washed in TD buffer (135 mmol l^{-1} NaCl, 5 mmol l^{-1} KCl, 25 mmol l^{-1} Tris-Cl, pH 7.6) and allowed to swell for 10 min in ice-cold hypotonic buffer (10 mmol l^{-1} NaCl, 1.5 mmol l^{-1} $CaCl_2$, 10 mmol l^{-1} Tris-Cl, pH 7.5, protease inhibitors). Cells were Dounce-homogenized (60 strokes), and MS buffer (210 mmol l^{-1} mannitol, 70 mmol l^{-1} sucrose, 5 mmol l^{-1} EDTA, 5 mmol l^{-1} Tris, pH 7.6) was added to stabilize the mitochondria. After removing nuclear contaminants, the supernatant was layered and spun at 4°C for 30 min at 55 200× *g*. Mitochondria were collected and resuspended in a final volume of 200 μl of MS buffer for specific experiments. The top layer was collected to obtain cytosolic and leaked nuclear and organelle proteins (free protein fraction).

Detection of oxygen in culture medium

The oxygen concentration of the medium was measured as previously described (Griffiths & Robinson, 1999). A 250 μm diameter fibre-optic sensor for the simultaneous quantification of P_{O_2} (OxyLite, Oxford Optronix, Oxford,

UK) was inserted in the culture medium during cell treatment. Short pulses of LED light were transmitted along this fibre-optic sensor to excite a platinum-based fluorophore in the sensor tip. The degree to which this fluorescent light is quenched is directly proportional to the number of oxygen molecules within the surrounding environment. The lifetime of fluorescence is inversely proportional to the concentration of dissolved oxygen and is interpreted to provide an absolute value for P_{O_2} in mmHg.

Oxygen availability assay

Oxygen availability assays were conducted as previously described (Hagen *et al.* 2003). In brief, cardiomyocytes or transformed African green monky kidney fibroblast cells were transfected with oxygen detection plasmids. Following 48 h transfection, the cells were subjected to specific treatments, as indicated in the figure legends. The *Renilla* luciferase substrate, coelenterazine-hcp, was added 5 min prior to the luminescence measurement at a final concentration of 5 μg ml^{-1}. Luminescence was measured by a microplate reader (Synergy 4, BioTek Instruments).

Nitric oxide (NO) measurement

NO was detected by a fluorescent NO-sensitive dye, 4,5-diaminofluorescein (DAF-2). Treated cells were incubated with DAF-2 diacetate (5 μM, Calbiochem) for 10 min at 37°C and subsequently washed. Single cell fluorescence was detected by a laser confocal microscope (A1R, Nikon, Tokyo, Japan). DAF-2 fluorescence was excited at 480 nm, and emitted fluorescence was measured at 540 nm.

Measurement of intracellular ATP and AMP levels

Cells were lysed with 500 μl of 0.2 mol l^{-1} $HClO_4$ and centrifuged at 5000 *g* for 10 min. The supernatant was neutralized with KOH on ice, centrifuged and filtered through a 10 kDa, followed by a 3 kDa, cutoff filter (Millipore, Billerica, MA, USA). The resulting filtrate was diluted 1:1 in 100 mmol l^{-1} phosphate buffer (pH 7.0) and analysed by HPLC (Waters, Milford, MA, USA) with an LC-18T reverse-phase column (Supelco, Bellefonte, PA, USA) at a flow rate of 1 ml min^{-1}, and the absorbance at 254 nm was recorded. Each elution peak was compared with AMP and ATP standards (Sigma) to confirm its identity (Dasgupta & Milbrandt, 2007).

AMPK activity assay

AMPK activity was determined as previously described (Kim *et al.* 2001). Cells were lysed with digitonin buffer (50 mmol l^{-1} Tris-HCl, pH 7.3, 50 mmol l^{-1} NaF, 30 mmol l^{-1} glycerol phosphate, 250 mmol l^{-1} sucrose, 1 mmol l^{-1} sodium metavanadate, and 0.4 mg ml^{-1} digitonin) on ice for 2 min. AMPK was partially purified from cell lysates by adding saturated ammonium sulfate to a final concentration of 35% (v/v) on ice for 15 min. AMPK activity was determined with these fractionated proteins in kinase assay buffer (62.5 mmol l^{-1} Hepes, pH 7.0, 62.5 mmol l^{-1} NaCl, 62.5 mmol l^{-1} NaF, 6.25 mmol l^{-1} sodium pyrophosphate, 1.25 mmol l^{-1} EDTA, 1.25 mmol l^{-1} EGTA, and 1 mmol l^{-1} dithiothreitol) containing 200 μmol l^{-1} AMP and an ATP mixture (200 μmol l^{-1} ATP and 1.5 μCi of [γ-^{32}P]ATP), with or without 250 μmol l^{-1} SAMS peptide (HMRSAMSGLHLVKRR) at 30°C for 10 min. The reaction was terminated by spotting the reaction mixture on phosphocellulose paper (P81), and the paper was extensively washed with 150 mmol l^{-1} phosphoric acid. The radioactivity was measured with a scintillation counter.

Reactive oxygen species (ROS) measurement

Intracellular ROS was detected with a fluorescent probe, dichlorodihydrofluorescein diacetate (H_2DCFDA) (Molecular Probes). Cardiomyocytes were cultured in 24-well plates to 80–90% confluence and dyed with a 1 mg ml^{-1} probe for 30 min in the dark at 37°C. Cells were then subjected to treatments as described in the figure legends. Fluorescence was measured at a 450 nm excitation and 530 nm emission wavelength by a microplate reader.

PHD activity assay

Prolyl hydroxylase (PHD) activity was determined as previously described (Oehme *et al.* 2004). Cell lysates were used as the source of prolyl hydroxylases. Hydroxylase reactions were carried out by using 1 μg (μl protein)$^{-1}$ of whole cell lysates in the presence of 100 μmol l^{-1} 2-oxoglutarate, 1 μmol l^{-1} $FeSO_4$ and 2 mmol l^{-1} ascorbate for 1 h at room temperature. After washing, 0.022 μg μl^{-1} thioredoxin-tagged pVHL in complex with elongins B and C (VBC) was allowed to bind to the hydroxylated peptide. Bound VBC complex was detected by rabbit anti-thioredoxin antibodies and secondary horseradish peroxidase-coupled anti-rabbit antibodies (Sigma) using the 3,3′,5,5′-tetramethyl-benzidine substrate kit (Pierce). The peroxidase reaction was stopped by adding H_2SO_4, and absorbance was determined at 450 nm in a microplate reader. Each experiment was calibrated to an internal standard curve using hydroxyproline (Pro^{564})-containing HIF-1α peptide (amino acids 556–574) and VBC complex.

Statistical analysis

Data are shown as mean ± S.E.M. Multiple group comparison was performed by one-way ANOVA followed by the Bonferroni procedure for comparison of means. Comparison between two groups was analysed by the two-tailed Student's *t* test or two-way ANOVA. Values of $P < 0.05$ were considered statistically significant.

Results

Intracellular oxygen assay

The MitRLuc-pcDNA3 plasmid was constructed by fusing the mitochondrial target sequence of MnSOD to the N-terminus of *Renilla* luciferase. The plasmid has been previously used to assay mitochondrial oxygen concentration by Drs Thilo Hagen (Hagen *et al.* 2003) and Jacques E. Riby (Riby *et al.* 2008). We performed relevant experiments to further validate this oxygen detection method.

The cell line derived from cervical cancer cells transfected with Mito Rluc-pcDNA3 were used to conduct an immunofluorescence experiment. The results suggested that the MitoRLuc protein was primarily localized in the mitochondria (Fig. 1*A*). Mit RLuc expression was nearly completely colocalized with the NDUFS2 and cytochrome *c* protein which are important components of the mitochondrial membrane respiratory chain (Procaccio *et al.* 1998; Loeffen *et al.* 2001; Waterhouse *et al.* 2001) (Fig. 1*B*, Supplemental Fig. S1 (available online only)). Moreover, Western blot analysis revealed that MitRLuc protein was only detected in the mitochondria fraction (Fig. 1*C*). *Renilla* luciferase activity was dependent on its substrates and O_2. At a given substrate concentration, *Renilla* luciferase activity merely correlates with O_2 availability. When HeLa cells were cultured in decreasing oxygen, *Renilla* luciferase activity was found to be decreased but up-regulation of HIF-1α expression (as a marker for the oxygen state) was detected simultaneously (Fig. 1*D* and *E*). This finding is also consistent with a previous report that *Renilla* luciferase activity reflects oxygen levels both in immunoprecipitated proteins and in intact cells (Hagen *et al.* 2003). Thus, we employed a *Renilla* luciferase reporter to detect intracellular oxygen availability.

β_2-AR stimulation increases intracellular oxygen availability in cardiomyocytes

In cardiomyocytes expressing the MitRLuc protein, the non-selective β-AR agonist isoproterenol (isoprenaline (ISO)) caused a rapid and significant increase in mitochondrial oxygen in a dose- and time-dependent manner. The maximal effect appeared at 1–10 μmol l^{-1} after 8 min of ISO stimulation (Fig. 2*A*). To determine which β-AR subtype is responsible for this effect, we used selective stimuli to activate either β_1-AR (combination of ISO with the β_2-AR antagonist ICI118551) or β_2-AR (ISO with the β_1-AR antagonist CGP20712A). ICI118551 (ICI) or CGP20712A (CGP) alone did not result in alteration of intracellular oxygen levels (data not shown). Selective stimulation of β_2-AR increased mitochondrial oxygen to a degree similar to ISO stimulation alone. Furthermore, the concentration of mitochondrial oxygen in β_2-AR-stimulated cells was significantly higher than that in unstimulated cells (Ctrl) (Fig. 2*B*). However, selective β_1-AR stimulation did not change mitochondrial oxygen. To exclude the possibility that ICI may exert an effect on β_1-AR, we also investigated the contraction amplitude of cardiomyocytes in response to β-AR stimulation. The result showed that β_1-AR inhibition by CGP remarkably decreased the contraction amplitude of cardiomyocytes compared with ISO treatment. However, ISO plus different concentrations of ICI did not affect the contraction amplitude compared with ISO stimulation alone, implicating that ICI treatment only inhibited β_2-AR-selective events but not β_1-AR selective events (Supplemental Fig. S2).

To further confirm this finding, we also stimulated cardiomyocytes using a selective β_2-AR agonist Zinterol (ZIN). This treatment resulted in an increase in mitochondrial oxygen similar to that of ISO stimulation, and the increase could be eliminated by ICI pretreatment (Fig. 2*C*). Through similar experiments, we also found that cytosolic oxygen was specifically regulated by β_2-AR activation (data not shown).

Because oxygen might diffuse from the culture medium into the cells, the possibility that the increase in intracellular oxygen is a result of diffusion from the extracellular environment was considered. OxyLite, a fibre-optic oxygen sensor, is a sensitive apparatus for the estimation of oxygen content (Griffiths & Robinson, 1999). It is sensitive to oxygen levels and, unlike P_{O_2} electrodes, does not consume oxygen, which could result in an artificially low P_{O_2} reading. We used the OxyLite method to assay oxygen concentration in culture medium. The result suggested that oxygen concentration in the culture medium remained unchanged at different time points (Fig. 2*D*), implicating that the change in intracellular oxygen is not due to diffusion from the extracellular environment. Taken together, β_2-AR activation specifically modulates intracellular oxygen availability.

β_2-AR stimulation specifically increases intracellular oxygen availability in another type of mammalian cell

In addition, we used another cell line to determine whether β_2-AR specifically regulates intracellular oxygen. COS7 cells were co-transfected with the oxygen assay plasmid

and β_1-AR or β_2-AR. Immunofluorescent staining revealed that β_1-AR and β_2-AR were mainly expressed on cell membranes (Fig. 3*A*). Endogenous expression of β_1-AR and β_2-AR proteins was difficult to detect in COS7 cells by Western blot; however, stable expression was found in transfected COS7 cells (Fig. 3*B*). ISO stimulation caused a significant increase in mitochondrial and cytosolic oxygen concentrations in cells expressing β_2-AR but not in cells expressing β_1-AR (Fig. 3*C*, Supplemental Fig. S3). This finding is consistent with the observed

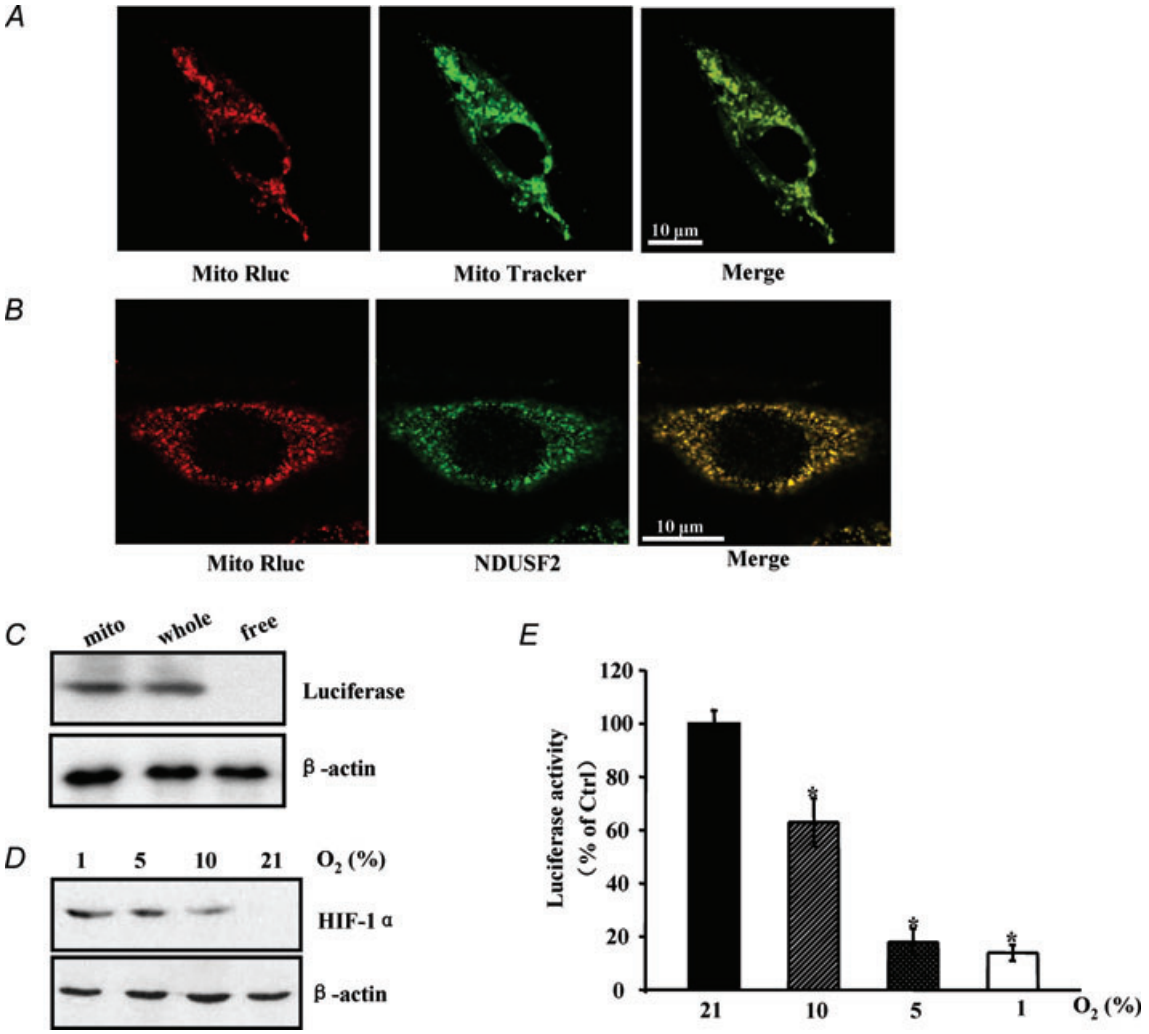

Figure 1. Evaluation of the method for intracellular oxygen detection
A, HeLa cells were transfected with the MitRLuc-pcDNA3 plasmid. After 48 h, the cells were stained with Mito-Tracker Green FM (Molecular Probes) to identify the localization of the mitochondria. Following mitochondrial labelling, cells were fixed with 4% paraformaldehyde, permeabilized with 0.1% Triton X-100 for 15 min, immunoblotted with luciferase antibody (Santa Cruz), and stained with Cy3-conjugated second antibody (Invitrogen). The sample was detected by confocal laser scanning microscopy. Merged images show the colocalization of the Mit-RLuc protein in mitochondria. *B*, HeLa cells were transfected with the MitRLuc-pcDNA3 plasmid. Forty-eight hours after transfection, the cells were fixed with 4% paraformaldehyde and permeabilized with 0.1% Triton X-100 for 15 min. After blocking with PBS supplemented with 5% bovine serum albumin for 30 min, the cells were immunolabelled with luciferase antibody followed by a Cy3-conjugated second antibody (Invitrogen). These cells were then immunoblotted with NDUFS2 (Santa Cruz) and FITC-labelled second antibody (Invitrogen). The samples were analysed using confocal laser microscopy. A representative image is shown. *C*, HeLa cells were transfected with MitRLuc-pcDNA3 for 48 h. Whole cell lysate, mitochondria (Mito) and free protein (whole cell lysate except the mitochondrial fraction) were prepared for the analysis of luciferase expression. *D*, HeLa cells were incubated at 21%, 10%, 5% and 1% O_2 for 8 h, and the induction of the HIF-1α protein was estimated by Western blot. β-Actin was used as a loading control. A representative image is shown. *E*, HeLa cells expressing MitRLuc-pcDNA3 were treated as in *D*. Luciferase activity was detected with a microplate reader. Decreased oxygen caused a concentration-dependent reduction in luciferase activity.

result in cardiomyocytes, and further confirms that β_2-AR stimulation plays a major role in the regulation of intracellular oxygen availability.

β_2-AR regulates oxygen availability through the β_2-AR–G_i–eNOS pathway

In the hearts of mammals including humans, stimulation of native cardiac β_2-AR activates both the stimulatory G protein and pertussis toxin (PTX)-sensitive G_i signalling pathways (Kuschel *et al.* 1999; Jo *et al.* 2002). G_s signalling leads to protein kinase A activation, phosphorylates the receptor and switches β_2-AR coupling from G_s to G_i (Tong *et al.* 2005). PTX, an inhibitor of G_i signalling, is a valuable tool to dissect G_i-dependent components of β_2-AR signalling (Danson *et al.* 2005). We found that PTX treatment completely abolished β_2-AR-mediated intracellular oxygen change, suggesting that G_i proteins

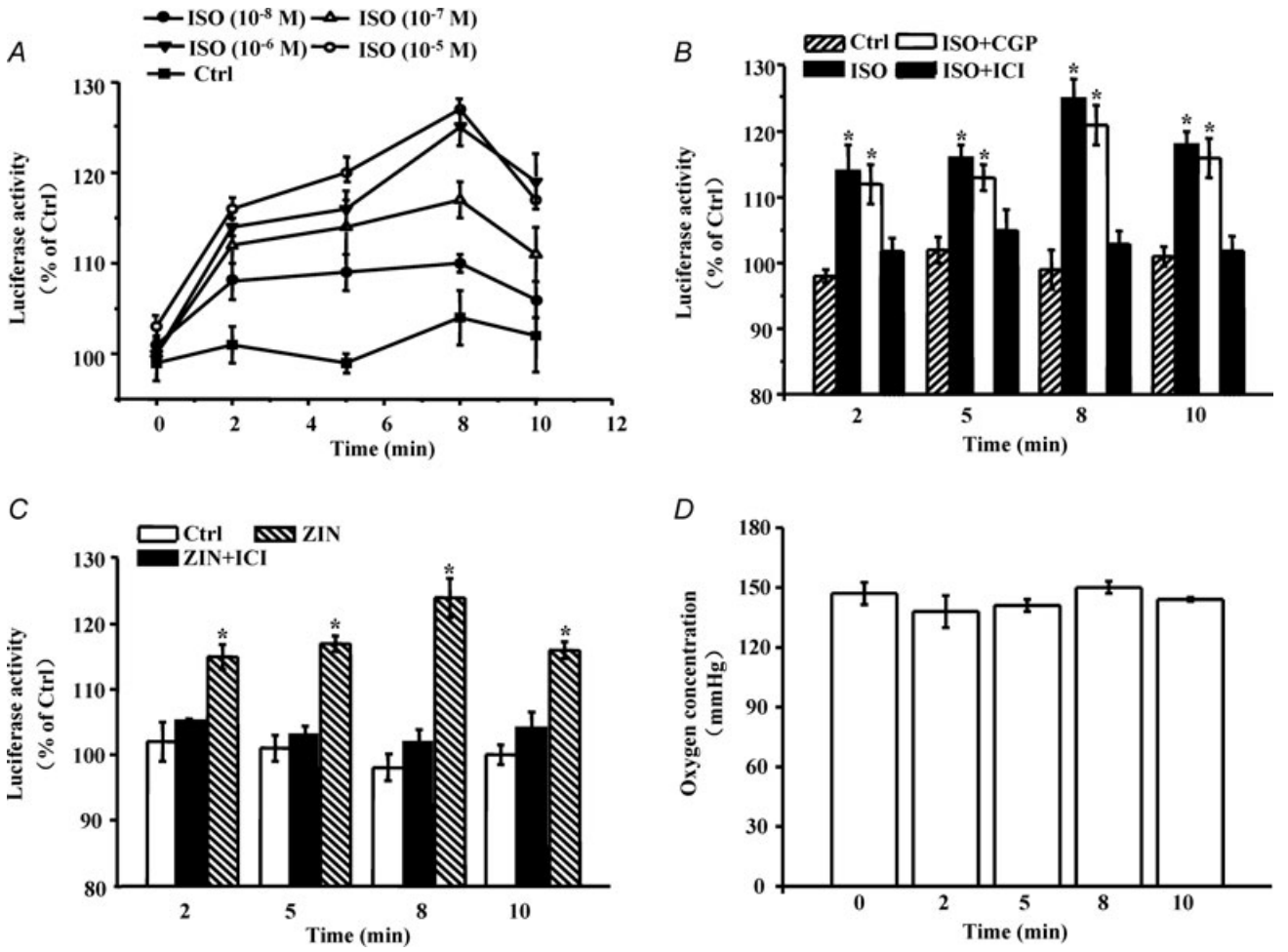

Figure 2. β_2-AR activation increases mitochondrial oxygen availability in cardiomyocytes
A, cardiomyocytes expressing the MitRLuc protein were treated with different concentrations of isoproterenol (isoprenaline, ISO) for 2, 5, 8 and 10 min. Following addition of the substrate coelenterazine (5 μg ml^{-1}), luminescence was determined with a microplate reader. *Renilla* luciferase activity was used to reflect the changes in intracellular oxygen. ISO regulated intracellular oxygen in a concentration- and time-dependent manner. *B* and *C*, cardiomyocytes expressing the MitRLuc protein were subjected to different pharmacological interventions to identify which receptor subtype was responsible for the change in intracellular oxygen. The drugs and doses were as follows: CGP20712A (CGP), a selective β_1-AR inhibitor, 300 nmol l^{-1}; ICI118551 (ICI), a selective β_2-AR inhibitor, 100 nmol l^{-1}; ISO, 1 μmol l^{-1}; Zinterol (ZIN), a selective β_2-AR agonist, 1 μmol l^{-1}. Cells were pretreated with antagonists for 15 min before the addition of agonists. Luminescence was determined as depicted in Methods. Values are expressed as a percentage compared to untreated cells. Asterisks (*) indicate $P < 0.05$ *versus* untreated cells (Ctrl). Error bars represent standard deviations. All data shown represent the mean ± S.E.M. for three separate experiments in duplicate. *D*, cardiomyocytes were treated with ISO (1 μmol l^{-1}) for the indicated time. The oxygen concentration in the culture medium was measured with a 250 μm-diameter fibre-optic sensor (OxyLite, Oxford Optronix, Oxford, UK). Data represent the means of three independent experiments. Error bars represent standard deviation.

are involved in the regulation of intracellular oxygen availability (Fig. 4*A*).

In addition, we found that ISO treatment caused rapid NO release in cardiomyocytes in a concentration-dependent manner (Supplemental Fig. S4), and NO release was specifically mediated by β_2-AR, but not β_1-AR activation (Fig. 4*B*). We asked whether NO generation is tightly associated with intracellular oxygen regulation. Carboxy-PTIO was employed to eliminate β_2-AR-mediated NO generation (Goldstein *et al.* 2003). Meanwhile, β_2-AR-mediated change in intracellular oxygen was nearly blocked by NO scavenging (Fig. 4*C*).

NO in the heart is generated by endothelial NO synthase (eNOS) in the endothelium and caveolae of cardiomyocytes, by neuronal NO synthase (nNOS) in the sarcoplasmic reticulum and possibly mitochondria, and by inducible NO synthase (iNOS) in the sarcoplasm under pathological situations (Moncada & Erusalimsky, 2002). Inhibition of nNOS or iNOS by *S*-methylthiocitrulline (SMTC, 100 nM) (Seddon *et al.* 2008) or L-canavanine (1 μM) (Mansart *et al.* 2006) had no effect on intracellular oxygen availability. However, inhibition of eNOS by *N*-nitro-L-arginine methyl ester (L-NAME, 500 nM) (Laursen *et al.* 2001) almost abolished the β_2-AR effect on intracellular oxygen, suggesting that eNOS-mediated NO release is responsible for the observed changes in intracellular oxygen (Fig. 4*D*, Supplemental Fig. S5).

β_2-AR stimulation increases the AMP/ATP ratio, AMPK activity, ROS production, and PHD activity

At steady state, approximately 90% of available oxygen is consumed by the mitochondria to produce ATP through oxidative phosphorylation (Rolfe & Brown, 1997). Cells have evolved protective mechanisms to enhance survival through the initiation of signalling pathways that sense alterations in cellular energy status. In cardiomyocytes, β_2-AR stimulation resulted in a reduction in ATP

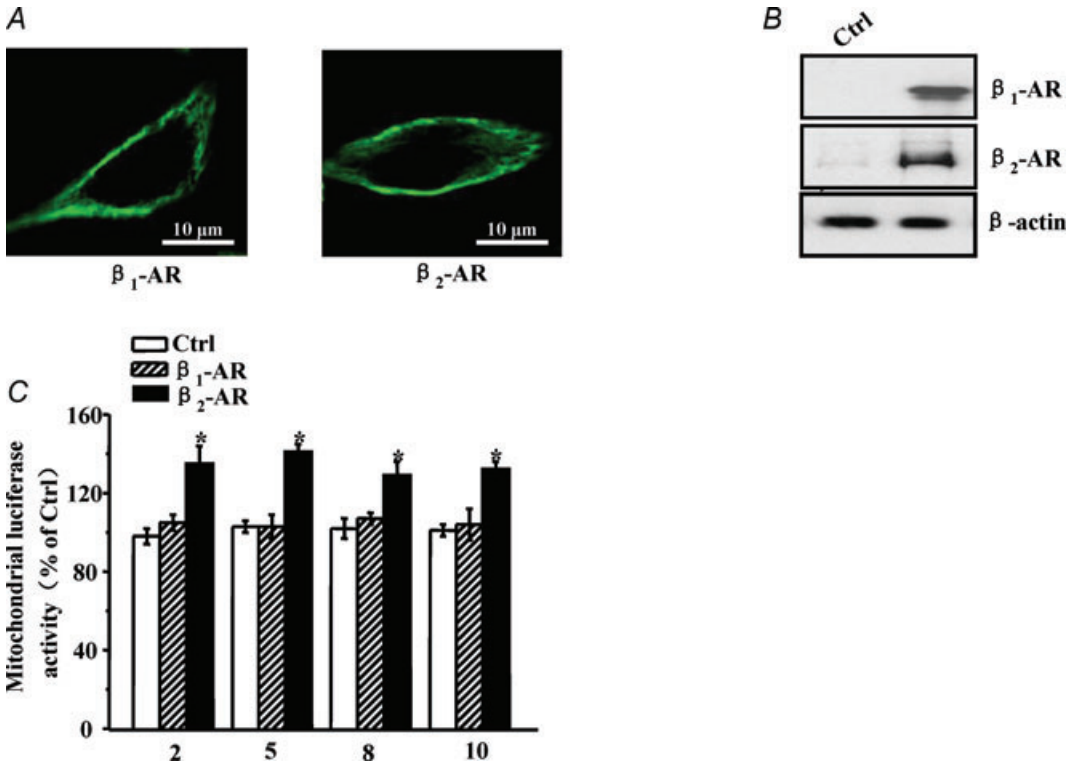

Figure 3. β_2-AR activation regulates mitochondrial oxygen availability in COS7 cells
A, COS7 cells were transfected with HA-tagged β_1-AR or β_2-AR plasmid for 48 h and then fixed with 4% paraformaldehyde and permeabilized with 0.1% Triton X-100 for 15 min. After blocking with PBS supplemented with 5% bovine serum for 30 min, cells were incubated with an HA primary antibody for 1 h at room temperature followed by an FITC-coupled secondary antibody for 30 min. Immunofluorescent staining was detected by confocal microscopy. A representative image is shown. *B*, COS7 cells were treated as in *A*, and untreated cells served as a control group (Ctrl). β_1-AR and β_2-AR expression was estimated by Western blot. β-Actin was used as a loading control. A representative experiment is shown. *C*, COS7 cells co-expressed the MitRLuc and β_1-AR or β_2-AR proteins for 48 h and were then stimulated with ISO for the indicated time to detect *Renilla* luciferase activity. Values are expressed as a percentage compared to unstimulated cells (Ctrl). Asterisks (*) indicate $P < 0.05$ *versus* unstimulated cells.

production but was accompanied by a rise in its precursor, AMP (Supplemental Fig. S6*A* and *B*). The AMP/ATP ratio was enhanced (Fig. 5*A*), which subsequently led to the activation of AMP-activated kinase (AMPK) (Fig. 5*B*). AMPK helps to maintain cellular energy homeostasis and ATP levels (Hardie, 2008). In addition, ROS generation is also a significant consequence of oxidative phosphorylation. Excessive or discontinuous oxygen consumption has significant pathological implications through ROS generation. We found that β_2-AR activation caused the inhibition of mitochondrial respiration and the increase in ROS production, implying that oxygen regulation and ROS production are encountered in physiological states (Fig. 5*C*).

In addition to its role in normal metabolism, oxygen is a crucial substrate for numerous enzymes, such as dioxygenase. Prolyl hydroxylase (PHD) is a dioxygenase that uses O_2 and α-ketoglutarate as substrates and generates CO_2 and succinate as by-products; this enzyme is sensitive to oxygen state. We found that PHD activity was specifically up-regulated by β_2-AR, but not β_1-AR stimulation (Fig. 5*D*). Alterations in PHD activity may transmit O_2-responsive signals to regulate cellular physiological events.

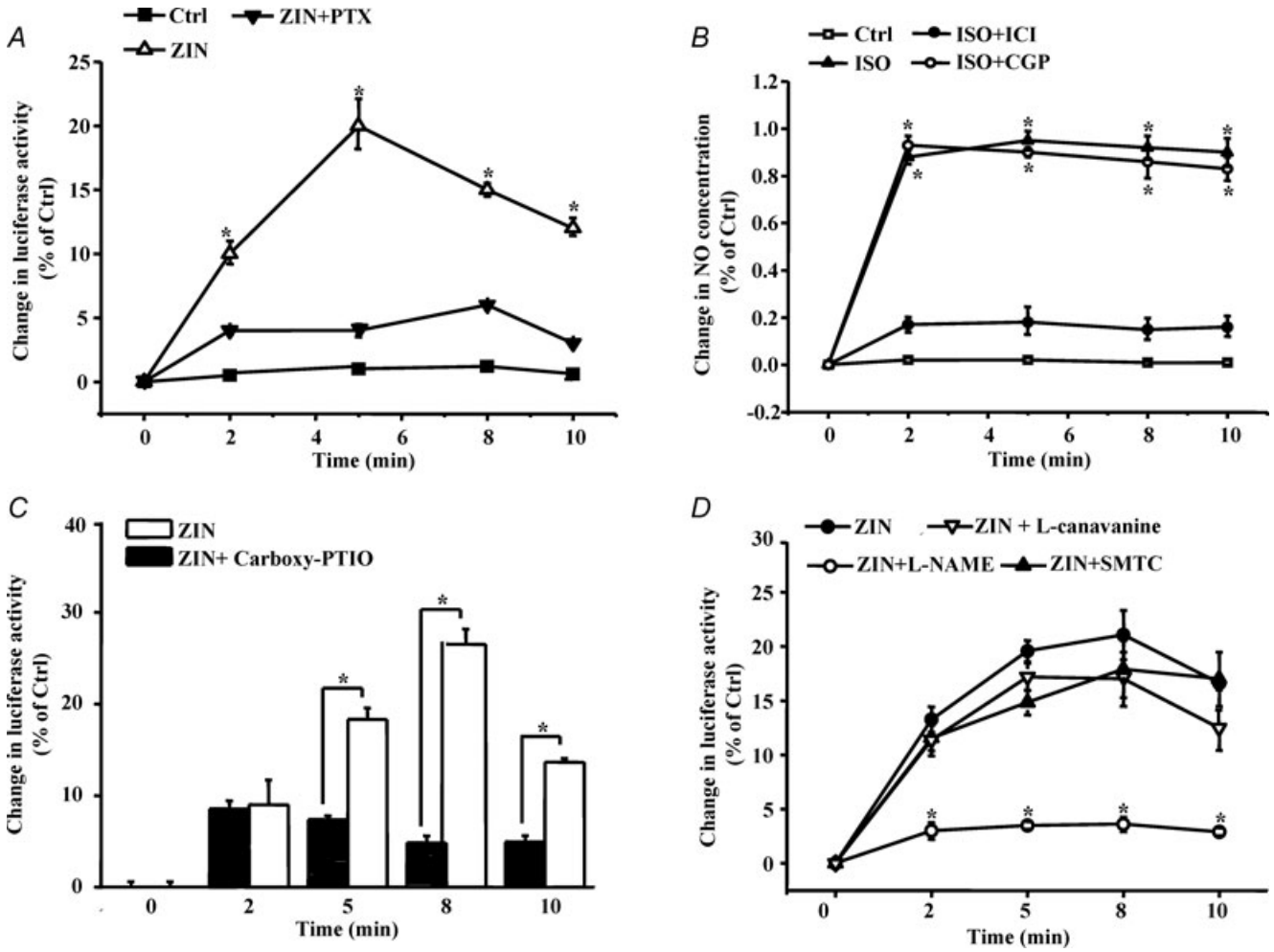

Figure 4. β_2-AR regulates oxygen availability through the β_2-AR–G_i–eNOS pathway
A, C and *D*, cardiomyocytes expressing the MitRLuc protein were pretreated with PTX (0.5 μg ml^{-1}, pretreated for 3 h at 37°C), carboxy-PTIO, and NOS inhibitors (pretreated for 30 min at 37°C), including L-NAME (500 nmol l^{-1}), SMTC (100 nmol l^{-1}) and L-canavanine (1 μmol l^{-1}). β-AR was stimulated by different treatments, and luciferase activity was then determined as described in Methods. The data are displayed as the degree of change relative to unstimulated cells (Ctrl). *B*, cardiomyocytes were loaded with a DAF-2 diacetate probe, pretreated with CGP or ICI for 15 min, and then stimulated with ZIN for the indicated time. DAF-2 fluorescence was excited at 480 nm, and emitted fluorescence was measured at 540 nm. Values are expressed as the relative change compared to untreated cells (Ctrl). Single cell fluorescence was detected by laser confocal microscopy. The data represent the means of three independent experiments, and each point represents the average of ten cells.

Discussion

Recent evidence suggests that as molecular oxygen became integral to biochemical pathways, many enzymatic reactions central to anoxic metabolism were effectively replaced in aerobic organisms (Raymond & Segre, 2006). Oxygen is required not only for metabolism processes but also for other biological functions. The vast majority of oxygen consumed is used by mitochondria for ATP production to facilitate normal physiological function at steady state. The remaining 'spare' oxygen is used for non-mitochondrial processes and is consumed by non-mitochondrial dioxygenases (Taylor, 2008). Thus, precise and rapid redistribution of intracellular oxygen is crucial for cell survival in response to sudden stimuli. β_2-AR activation specifically results in an increase in intracellular oxygen availability. The phenomenon occurs within 10 min and can be considered as an acute response.

β_2-AR is a prototypical GPCR with distinct localization within membrane microdomains (DiPilato & Zhang, 2009) and is coupled with both the G_i and G_s proteins. Its activation increases cardiac contraction through G_s-mediated signalling and reduces cardiac contraction or initiates anti-apoptotic signalling via the G_i-coupled signalling pathway (Tong *et al.* 2005). In the study, we found that the G_i protein plays an important role in the regulation of intracellular oxygen. This finding further extends the function of the G_i protein in cells.

Lipid rafts and caveolae are typical membrane microdomains that spatially organize GPCR signalling molecules to promote kinetically favourable interactions to facilitate transduction (Ostrom & Insel, 2004). G proteins undergo signal-dependent trafficking into or out of lipid rafts. Rafts function as sites for G-protein trafficking and internalization as well as platforms for

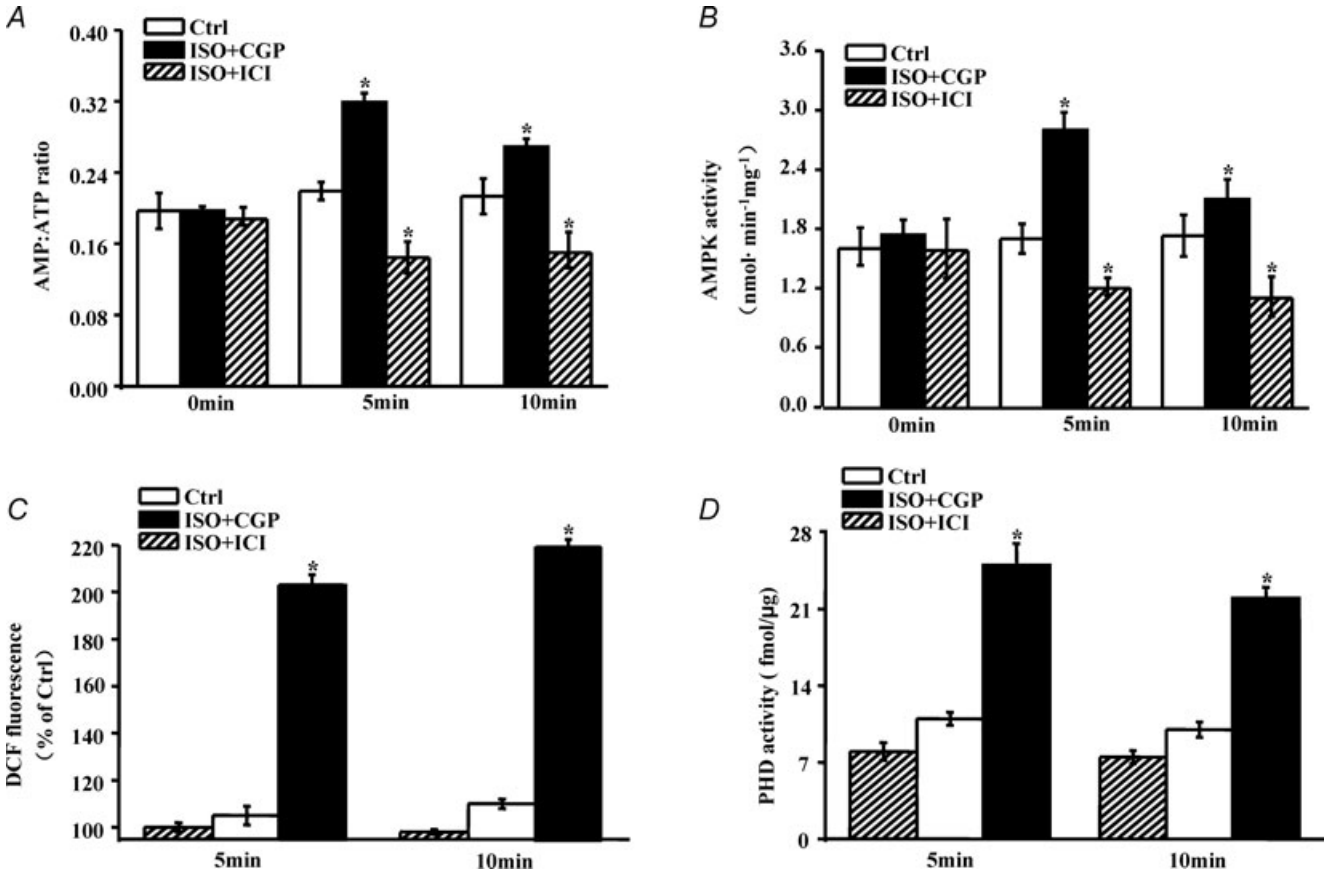

Figure 5. β_2-AR activation increases the AMP/ATP ratio, AMPK activity, ROS production and PHD activity
A, B and *C*, cardiomyocytes were pretreated with ICI or CGP for 15 min and then stimulated with ISO for the indicated time. Intracellular ATP and AMP levels were measured by HPLC. Results are expressed as AMP/ATP ratios at different time points. AMPK was purified from cell lysates. AMPK activity was determined as described in Methods through measurement of the radioactivity of an enzymatic reaction. Intracellular ROS levels were measured using a fluorescent probe H_2DCFDA. The data are expressed as a percentage compared to the untreated group (Ctrl). *D*, cardiomyocytes were treated as in *A*, and whole cell lysates were subjected to an *in vitro* PHD activity assay using the wild-type HIF-1α (556–574) peptide. The specific procedure is described in Methods. All data shown represent the mean ± S.E.M. for three separate experiments in duplicate. Asterisks (*) indicate $P < 0.05$ *versus* untreated cells (Ctrl) for the corresponding time point.

signalling (Allen *et al.* 2006). In addition, caveolae are reported to regulate the physiological signalling of β_2-AR subtypes in cardiomyocytes and may influence the coupling of $G\alpha_i$ (Rybin *et al.* 2000; Xiang *et al.* 2002). We suppose that this membrane microdomain also acts in intracellular oxygen regulation. In a preliminary experiment, we found that once caveolae were destroyed by methyl-β-cyclodextrin (MβC, 1 mM), β_2-AR stimulation did not change the level of intracellular oxygen, implicating that localization of β_2-AR to caveolae is required. Furthermore, the concentration of intracellular oxygen was not different among PTX-pretreated, MβC-pretreated, or PTX plus MβC-pretreated cells in response to β_2-AR stimulation (Supplemental Fig. S7). These data also suggest that caveolae and the G_i protein co-exist within the same pathway to regulate intracellular oxygen. In addition, other studies report that $G\alpha_s$ is also related to lipid rafts/caveolae in cardiomyocytes, and this localization might modulate $G\alpha_s$-coupled GPCR signalling (Rybin *et al.* 2000; Head *et al.* 2006). Allen *et al.* first used a simplified model system in C6 glioma cells to clarify the underlying mechanisms (Allen *et al.* 2009). They revealed that caveolin-1 and lipid microdomains act in $G\alpha_s$ trafficking and signalling. $G\alpha_s$ in lipid rafts/caveolae is removed from membrane signalling cascades, and caveolins might dampen global $G\alpha_s$–adenylyl cyclase–cAMP signalling. This finding indirectly supports our finding: in response to β_2-AR stimulation, lipid rafts/caveolae are involved in G_s inhibition, which may aid in the β_2-AR coupling switch from G_s to G_i protein. G_i proteins then participate in the regulation of intracellular oxygen and in turn, initiate other signalling pathways.

ATP-dependent signalling is a protective mechanism for cell survival (Towler & Hardie, 2007). β_2-AR activation causes a decrease in ATP and an increase in AMP. An increase in the AMP/ATP ratio leads to the activation of AMP-activated kinase (AMPK). The AMPK pathway is involved in the beneficial effects of exercise and represents a new therapeutic target for metabolic diseases, such as diabetes. AMPK activation promotes catabolic pathways, including glucose transport, gluconeogenesis, respiration and the use of alternative energy sources to oxygen, and downregulates anabolic pathways. These events are critical in maintaining cellular ATP levels. Furthermore, rapid activation of AMPK occurs in conditions of myocardial ischaemia. AMPK activation increases energy production and inhibits apoptosis, thereby protecting the heart during ischaemic stress (Dyck & Lopaschuk, 2006). In summary AMPK activation plays a beneficial role in cardiovascular protection.

The efficient respiratory chain functions within a narrow range of O_2 concentrations (Semenza, 2007*b*). Oxygen changes trigger mitochondrial respiratory chain dysfunction. A fraction of electrons escape the respiratory chain and combine with O_2 prematurely, resulting in the generation of ROS. β_2-AR activation causes the inhibition of the respiratory chain and an increase in ROS production. ROS has been reported to transmit intracellular signalling events (Ushio-Fukai, 2006) and leads to the modulation of protein function and protein–protein interactions (Stadtman, 2006). Moreover, ROS formation is required for β_2-AR signal transduction and stabilizes the active receptor conformations by redox-mediated modification of cysteine residues of the receptor and/or $G\alpha$ protein (Moniri & Daaka, 2007). Thus, ROS generation is also helpful for fine-tuning β_2-AR signalling.

In addition, β_2-AR activation specifically enhances the activity of PHD proteins. More importantly, this trend in PHD activity is consistent with changes in intracellular oxygen. PHD proteins are essential sensors of cellular oxygen state and mediate O_2-responsive signals through the modification of the target proteins with which they interact. One subtype, EGLN3, is most abundant in cardiac and smooth muscle (Xie *et al.* 2009). EGLN3 interacts directly with β_2-AR to serve as an endogenous β_2-AR prolyl hydroxylase and consequently affects receptor degradation and down-regulation. β_2-AR signalling modulates intracellular oxygen availability, and the altered oxygen level triggers a change in PHD activity. PHD activity has feedback effects on the responsiveness of β_2-AR signalling. β_2-AR, O_2 and PHD constitute a rapid, accurate and complicated signalling network that responds to various stimuli, and oxygen acts as a mediator to regulate this signalling network.

In conclusion, β_2-AR activation specifically modulates intracellular oxygen availability. This regulation is mediated by the β_2-AR–G_i–eNOS pathway, which consequently affects AMPK activity, ROS generation and PHD activity. These findings provide insight into the regulation of oxygen homeostasis, broaden the scope of β_2-AR functions, and may have crucial implications for β_2-AR regulation.

References

Allen JA, Halverson-Tamboli RA & Rasenick MM (2006). Lipid raft microdomains and neurotransmitter signaling. *Nat Rev Neurosci* **8**, 128–140.

Allen JA, Yu JZ, Dave RH, Bhatnagar A, Roth BL & Rasenick MM (2009). Caveolin-1 and lipid microdomains regulate G_s trafficking and attenuate G_s/adenylyl cyclase signaling. *Mol Pharmacol* **76**, 1082–1093.

Danson EJF, Zhang YH, Sears CE, Edwards AR, Casadei B & Paterson DJ (2005). Disruption of inhibitory G-proteins mediates a reduction in atrial β-adrenergic signaling by enhancing eNOS expression. *Cardiovasc Res* **67**, 613–623.

Dasgupta B & Milbrandt J (2007). Resveratrol stimulates AMP kinase activity in neurons. *Proc Natl Acad Sci U S A* **104**, 7217–7222.

DiPilato LM & Zhang J (2009). The role of membrane microdomains in shaping β_2-adrenergic receptor-mediated cAMP dynamics. *Mol Biosyst* **5**, 832–837.

Drummond GB (2009). Reporting ethical matters in *The Journal of Physiology*: standards and advice. *J Physiol* **587**, 713–719.

Dyck JRB & Lopaschuk GD (2006). AMPK alterations in cardiac physiology and pathology: enemy or ally? *J Physiol* **574**, 95–112.

Goldstein S, Russo A & Samuni A (2003). Reactions of PTIO and carboxy-PTIO with $^{\cdot}NO$, $^{\cdot}NO_2$, and $O_2^{-}\cdot$. *J Biol Chem* **278**, 50949–50955.

Griffiths JR & Robinson SP (1999). The OxyLite: a fibre-optic oxygen sensor. *Brit J Radiol* **72**, 627–630.

Hagen T, Taylor CT, Lam F & Moncada S (2003). Redistribution of intracellular oxygen in hypoxia by nitric oxide: effect on HIF1α. *Science* **302**, 1975–1978.

Hardie DG (2008). AMPK: a key regulator of energy balance in the single cell and the whole organism. *Int J Obes* **4**, S7–S12.

Head BP, Patel HH, Roth DM, Murray F, Swaney JS, Niesman IR, Farquhar MG & Insel PA (2006). Microtubules and actin microfilaments regulate lipid raft/caveolae localization of adenylyl cyclase signaling components. *J Biol Chem* **281**, 26391–26399.

Iaccarino G, Ciccarelli M, Sorriento D, Galasso G, Campanile A, Santulli G, Cipolletta E, Cerullo V, Cimini V, Altobelli GG, Piscione F, Priante O, Pastore L, Chiariello M, Salvatore F, Koch WJ & Trimarco B (2005). Ischemic neoangiogenesis enhanced by β_2-adrenergic receptor overexpression: a novel role for the endothelial adrenergic system. *Circ Res* **97**, 1182–1189.

Iaccarino G, Cipolletta E, Fiorillo A, Annecchiarico M, Ciccarelli M, Cimini V, Koch WJ & Trimarco B (2002). β_2-Adrenergic receptor gene delivery to the endothelium corrects impaired adrenergic vasorelaxation in hypertension. *Circulation* **106**, 349–355.

Insel PA (1996). Adrenergic receptors – evolving concepts and clinical implications. *N Engl J Med* **334**, 580–585.

Johnson M (1998). The β-adrenoceptor. *Am J Respir Crit Care Med* **158**, S146–S153.

Jo SH, Leblais V, Wang PH, Crow MT & Xiao RP (2002). Phosphatidylinositol 3-kinase functionally compartmentalizes the concurrent G_s signaling during β_2-adrenergic stimulation. *Circ Res* **91**, 46–53.

Kim J, Yoon MY, Choi SL, Kang I, Kim SS, Kim YS, Choi YK & Ha J (2001) Effects of stimulation of AMP-activated protein kinase on insulin-like growth factor 1- and epidermal growth factor-dependent extracellular signal-regulated kinase pathway. *J Biol Chem* **276**, 19102–19110.

Kuschel M, Zhou YY, Cheng H, Zhang SJ, Chen Y, Lakatta EG & Xiao RP (1999). G_i protein-mediated functional compartmentalization of cardiac β_2-adrenergic signaling. *J Biol Chem* **274**, 22048–22052.

Laursen JB, Somers M, Kurz S, McCann L, Warnholtz A, Freeman BA, Tarpey M, Fukai T & Harrison DG (2001). Endothelial regulation of vasomotion in apoE-deficient mice: implications for interactions between peroxynitrite and tetrahydrobiopterin. *Circulation* **103**, 1282–1288.

Lefkowitz RJ, Rockman HA & Koch WJ (2000). Catecholamines, cardiac β-adrenergic receptors, and heart failure. *Circulation* **101**, 1634–1637.

Loeffen J, Elpeleg O, Smeitink J, Smeets R, Stöckler-Ipsiroglu S, Mandel H, Sengers R, Trijbels F & van den Heuvel L (2001). Mutations in the complex I NDUFS2 gene of patients with cardiomyopathy and encephalomyopathy. *Ann Neurol* **49**, 195–201.

Mansart A, Bollaert PE, Giummelly P, Capdeville-Atkinson C & Atkinson J (2006). Effects of dexamethasone and L-canavanine on the intracellular calcium-contraction relation of the rat tail artery during septic shock. *Am J Physiol Heart Circ Physiol* **291**, H1177–H1182.

Mieno S, Watanabe F, Sawa Y & Horimoto H (2005). Gene transfer of β_2 adrenergic receptor enhances cardioprotective effects of ischemic preconditioning in rat hearts after myocardial infarction. *Interact Cardiovasc Thorac Surg* **4**, 163–167.

Moncada S & Erusalimsky JD (2002). Does nitric oxide modulate mitochondrial energy generation and apoptosis? *Nat Rev Mol Cell Biol* **3**, 214–220.

Moniri NH & Daaka Y (2007). Agonist-stimulated reactive oxygen species formation regulates 2-adrenergic receptor signal transduction. *Biochem Pharmacol* **74**, 64–73.

Oehme F, Jonghaus W, Narouz-Ott L, Huetter J & Flamme I (2004). A nonradioactive 96-well plate assay for the detection of hypoxia-inducible factor prolyl hydroxylase activity. *Anal Biochem* **330**, 74–80.

Ostrom RS & Insel PA (2004). The evolving role of lipid rafts and caveolae in G protein-coupled receptor signaling: implications for molecular pharmacology. *Br J Pharmacol* **143**, 235–245.

Procaccio V, de Sury R, Martinez P, Depetris D, Rabilloud T, Soularue P, Lunardi J & Issartel JP (1998). Mapping to 1q23 of the human gene (NDUFS2) encoding the 49-kDa subunit of the mitochondrial respiratory Complex I and immunodetection of the mature protein in mitochondria. *Mamm Genome* **9**, 482–484.

Raymond J & Segre D (2006). The effect of oxygen on biochemical networks and the evolution of complex life. *Science* **311**, 1764–1767.

Riby JE, Firestone GL & Bjeldanes LF (2008). 3,3-Diindolylmethane reduces levels of HIF-1 and HIF-1 activity in hypoxic cultured human cancer cells. *Biochem Pharmacol* **75**, 1858–1867.

Rockman HA, Koch WJ & Lefkowitz RJ (2002). Seven-transmembrane-spanning receptors and heart function. *Nature* **415**, 206–212.

Rolfe DF & Brown GC (1997). Cellular energy utilization and molecular origin of standard metabolic rate in mammals. *Physiol Rev* **77**, 731–758.

Rybin VO, Xu X, Lisanti MP & Steinberg SF (2000). Differential targeting of β-adrenergic receptor subtypes and adenylyl cyclase to cardiomyocyte caveolae. A mechanism to functionally regulate the cAMP signaling pathway. *J Biol Chem* **275**, 41447–41457.

Salpeter SR, Ormiston TM & Salpeter EE (2004). Cardiovascular effects of β-agonists in patients with asthma and COPD. *Chest* **125**, 2309–2321.

Seddon MD, Chowienczyk PJ, Brett SE, Casadei B & Shah AM (2008). Neuronal nitric oxide synthase regulates basal microvascular tone in humans in vivo. *Circulation* **117**, 1991–1996.

Semenza GL (2007*a*). Life with oxygen. *Science* **318**, 62–64.

Semenza GL (2007*b*). Oxygen-dependent regulation of mitochondrial respiration by hypoxia-inducible factor 1. *Biochem J* **405**, 1–10.

Stadtman ER (2006). Protein oxidation and aging. *Free Radical Res* **40**, 1250–1258.

Taylor CT (2008*a*). Mitochondria, oxygen sensing, and the regulation of HIF-2α. Focus on "Induction of HIF-2α is dependent on mitochondrial O_2 consumption in an O_2-sensitive adrenomedullary chromaffin cell line". *Am J Physiol Cell Physiol* **294**, C1300–C1302.

Taylor CT (2008*b*). Mitochondria and cellular oxygen sensing in the HIF pathway. *Biochem J* **409**, 19–26.

Tong H, Bernstein D, Murphy E & Steenbergen C (2005). The role of β-adrenergic receptor signaling in cardioprotection. *FASEB J* **19**, 983–985.

Towler MC & Hardie DG (2007). AMP-activated protein kinase in metabolic control and insulin signaling. *Circ Res* **100**, 328–341.

Ushio-Fukai M (2006). Localizing NADPH oxidase-derived ROS. *Sci STKE* **22**, re8.

Waterhouse NJ, Goldstein JC, Von Ahsen O, Schuler M, Newmeyer DD & Green DR (2001). Cytochrome c maintains mitochondrial transmembrane potential and ATP generation after outer mitochondrial membrane permeabilization during the apoptotic process. *J Cell Biol* **153**, 319–328.

Xiang Y, Rybin VO, Steinberg SF & Kobilka B (2002). Caveolar localization dictates physiologic signaling of β_2-adrenoceptors in neonatal cardiac myocytes. *J Biol Chem* **277**, 34280–34286.

Xie L, Xiao K, Whalen EJ, Forrester MT, Freeman RS, Fong G, Gygi SP, Lefkowitz RJ & Stamler JS. (2009). Oxygen-regulated β_2-adrenergic receptor hydroxylation by EGLN3 and ubiquitylation by pVHL. *Sci Signal* **2**, ra33.

Author contributions

Y.-H.C. designed the research; J.L., B.Y., Z.H., Y.L., J.X., Y.S., Y.L., D.L., Y.Z. and J.S. performed the research; J.L., B.Y., Z.H., L.P., Z.-N.Z. and J.C. analysed the data; J.L., B.Y., Z.H. and Y.-H.C. wrote the paper. All authors read and approved the manuscript for publication.

Acknowledgements

This work was supported by the National Science Fund of China (30425016, 30330290 and 30470961), the '973' Program Fund of China (2007CB512100), the '863' Program Fund of China (2007AA02Z438), the Program Fund for Shanghai Subject Chief Scientists, the Program Fund for Innovative Research Teams by the Ministry of Education of China (Y.-H.C.), the Shanghai Pujiang Program Fund (07PJ14058, L.P.), the '973' Program Fund of China (2006CB504100, Z.-N.Z.), and the National Science Fund of China (30528011, J.C.). The authors have no conflicts of interest to disclose.